Supplementary information of

A cleaner snow future mitigates Northern Hemisphere snowpack loss from warming

Dalei Hao[1*], Gautam Bisht[1], Hailong Wang[1], Donghui Xu[1], Huilin Huang[1], Yun Qian[1] and L. Ruby Leung[1*]

[1]Atmospheric Sciences and Global Change Division, Pacific Northwest National Laboratory, Richland, WA, USA

This PDF file contains:

Supplementary Figures 1-7

Supplementary Tables 1-3

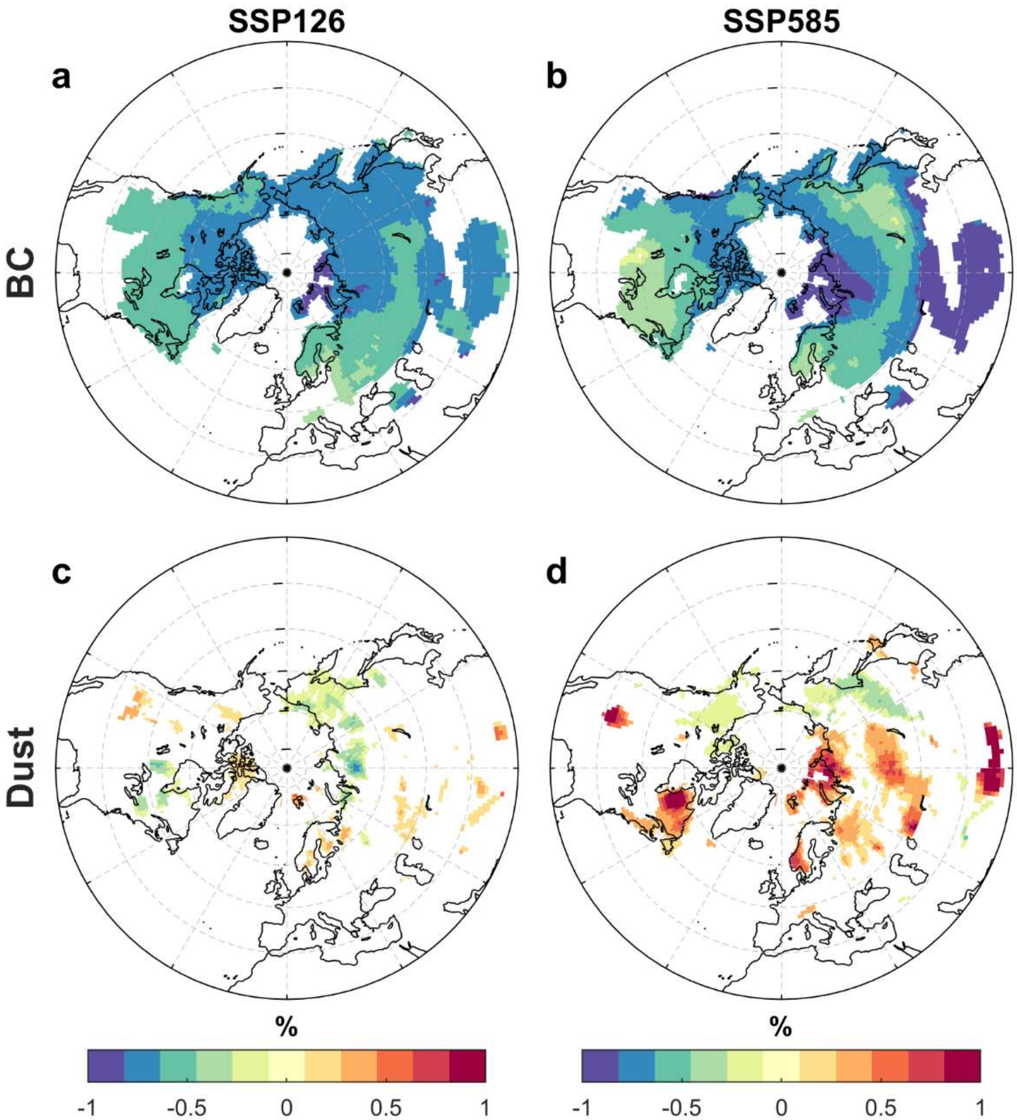

Figure S1| Future trends of BC and dust deposition from 2015-2100 over the Northern Hemisphere (NH). a,b Spatial pattern of the relative Sen's slopes of BC deposition under SSP126 and SSP585. **c,d** Spatial pattern of the relative Sen's slopes of dust deposition under SSP126 and SSP585**.** Here, the ensemble mean of seven CMIP6 model outputs from December to May are used to calculate the Sen's slope. The relative Sen's slope is calculated as the ratio of Sen's slope to the historical (1995-2015) average deposition rates. In each panel, grids without significant increasing or decreasing trends ($p>0.05$ in the MK test) or where SWE is smaller than 5 mm are masked.

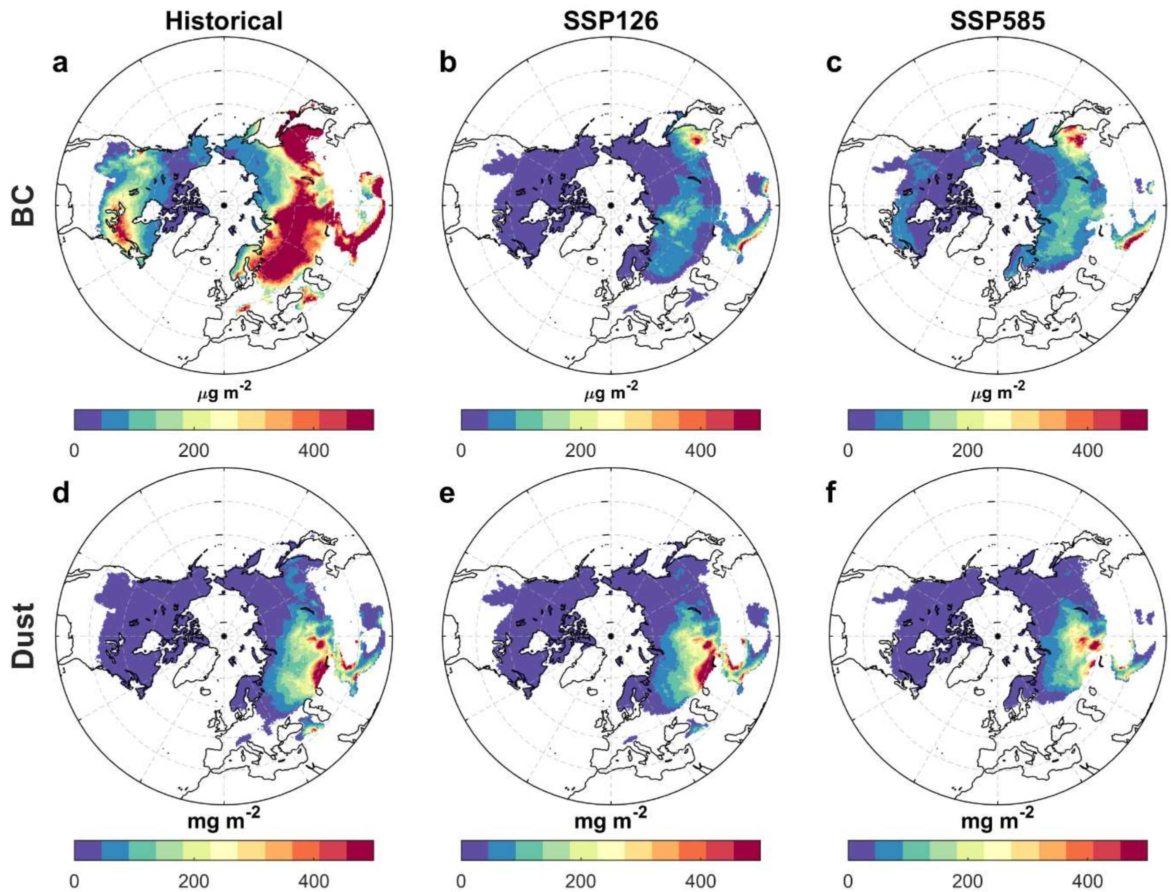

Figure S2| Spatial patterns of historical and future surface concentrations of BC and dust in the top snow layer over the NH. a,d Historical (1995-2014) and **b,c,e,f** future (2081-2100) spatial patterns of the surface concentration of BC and dust under SSP126 and SSP585. Historical and future surface concentrations are calculated based on ELM outputs for December to May. In each panel, the grids where SWE is smaller than 5 mm are masked.

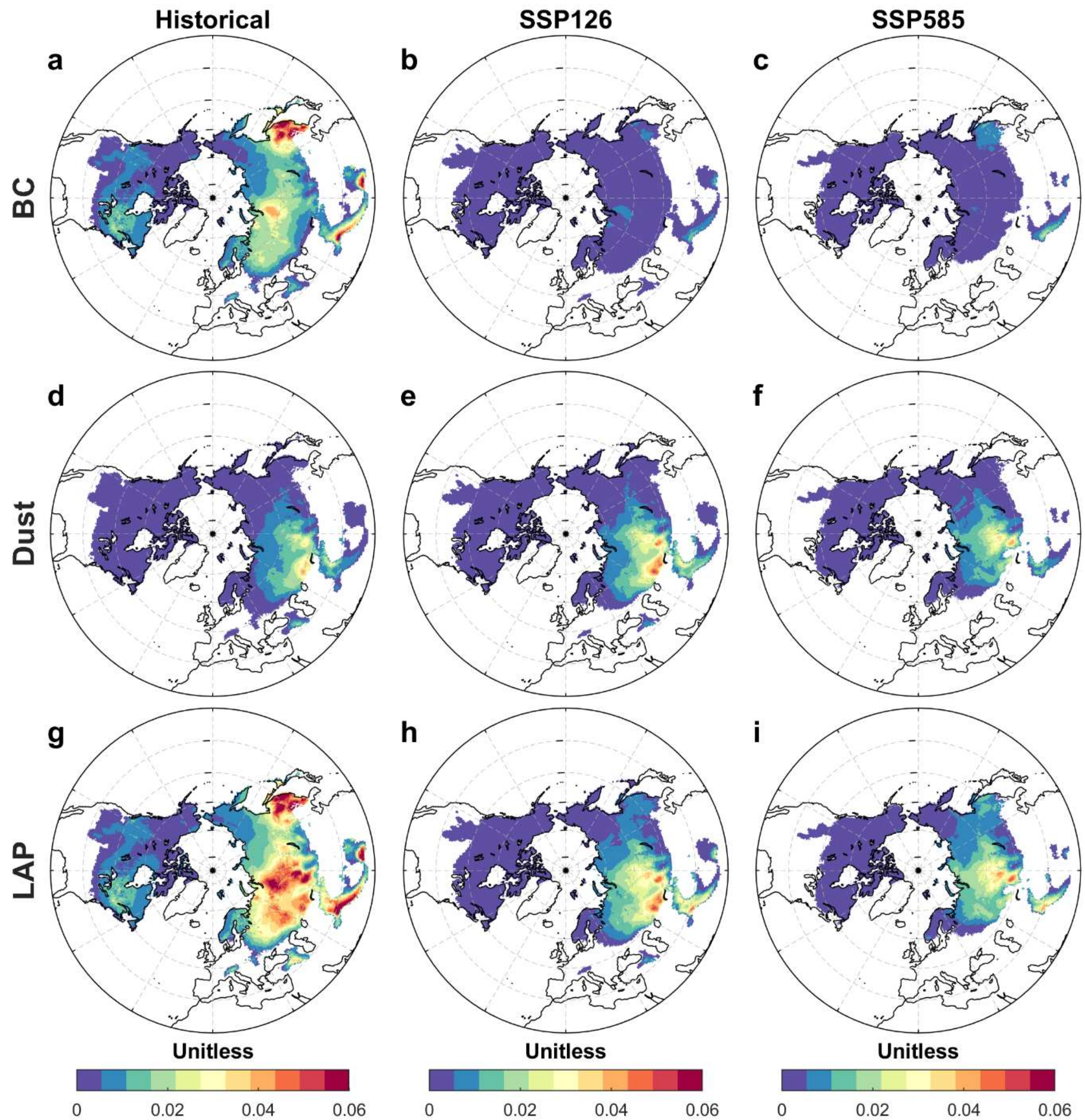

Figure S3| Spatial patterns of historical and future snow albedo reduction caused by BC, dust, and LAPs (the sum of BC and dust) over the NH. a,d,g Historical (1995-2014) and **b,c,e,f,h,i** future (2081-2100) spatial patterns of RFs under SSP126 and SSP585. Historical and future snow albedo reductions are calculated based on ELM outputs for December to May. In each panel, grids where SWE is smaller than 5 mm are masked.

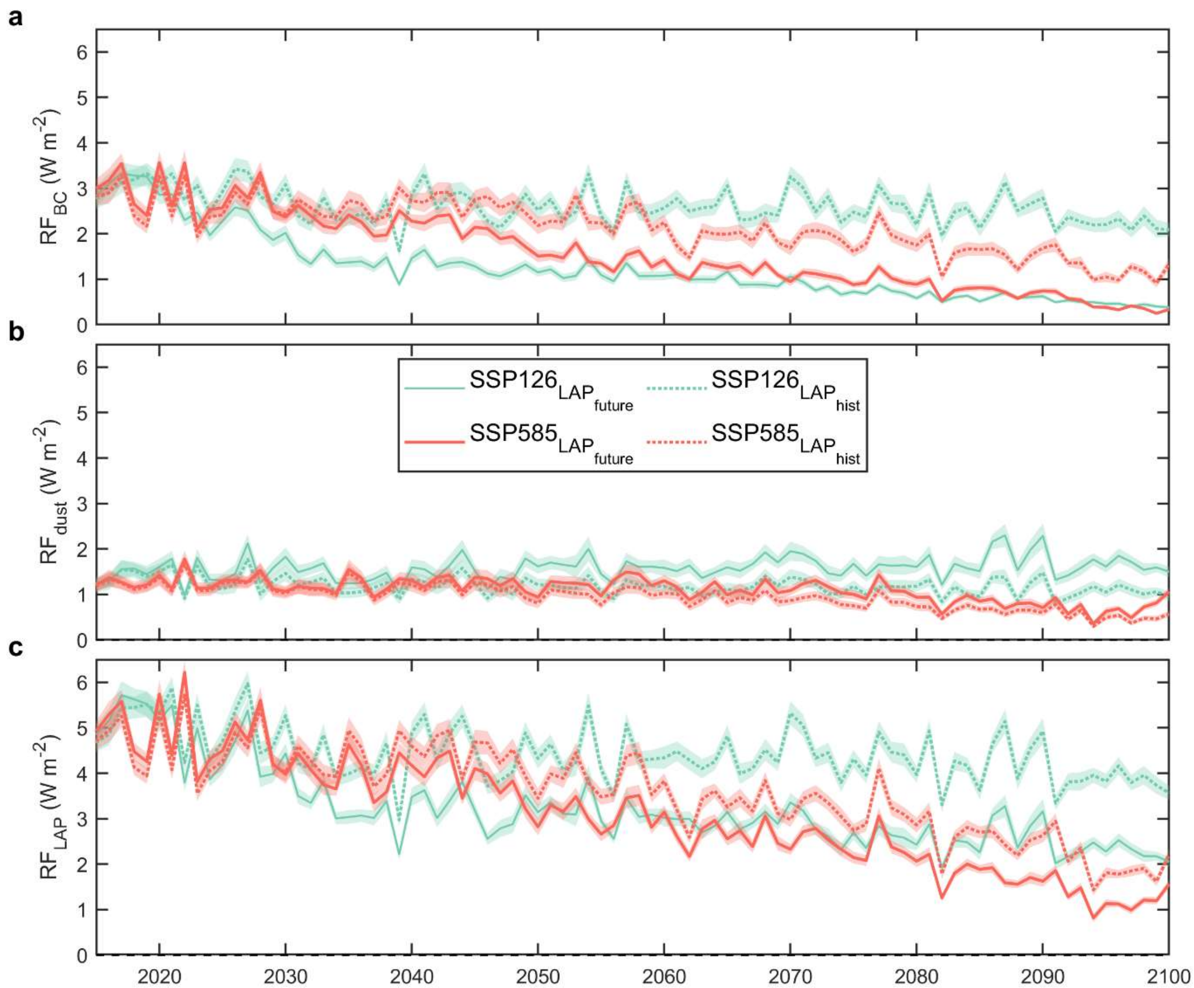

Figure S4| Time series of average surface radiative forcings (RF) from December to May caused by (a) BC, (b) dust, and (c) LAP (the sum of BC and dust) over snow-covered Tibetan Plateau (TP) regions (where the average SWE exceeds 5 mm in the historical period of 1995-2014) under SSP126 and SSP585. For each panel, the solid and dotted lines represent future simulations with and without future LAP change, with respect to the subscript of LAP_{future} and LAP_{hist} seen in the legend.

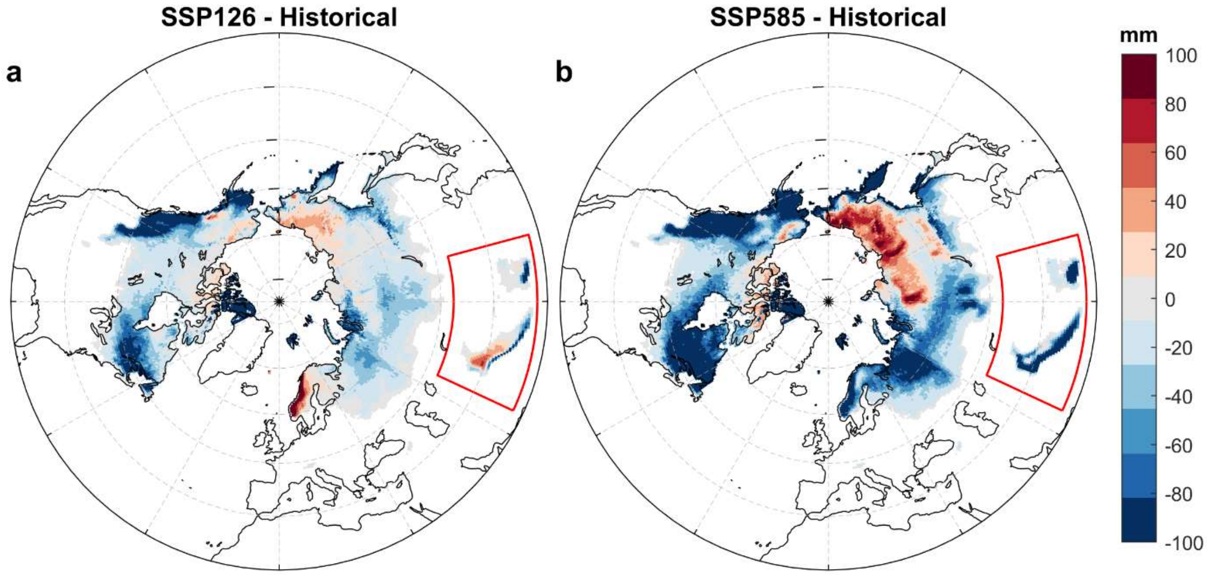

Figure S5| Spatial differences between future (2081-2100) and historical (1995-2014) SWE in April under (a) SSP126 and (b) SSP585. Grids where the average SWE exceeds 5 mm in the historical period of 1995-2014 are masked**.**

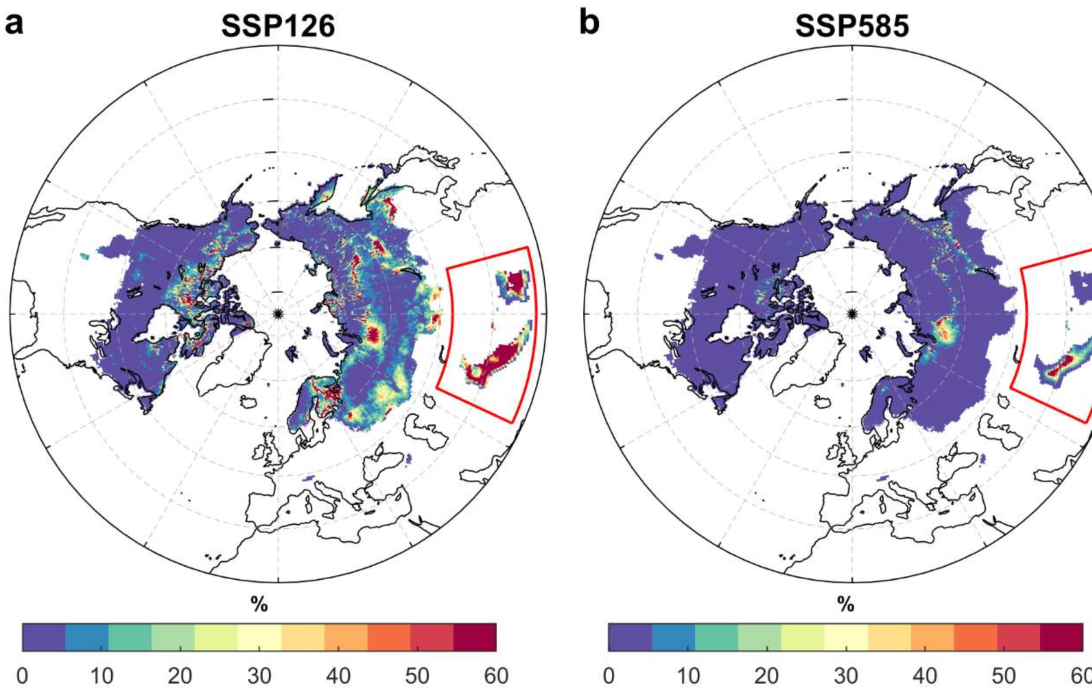

Figure S6| Spatial distributions of the contribution (δ_{LAP}, see Methods for its definition) of future LAP change to mitigating snowpack loss under (a) SSP126 and (b) SSP585. Grids where the average SWE exceeds 5 mm in the historical period of 1995-2014 are masked.

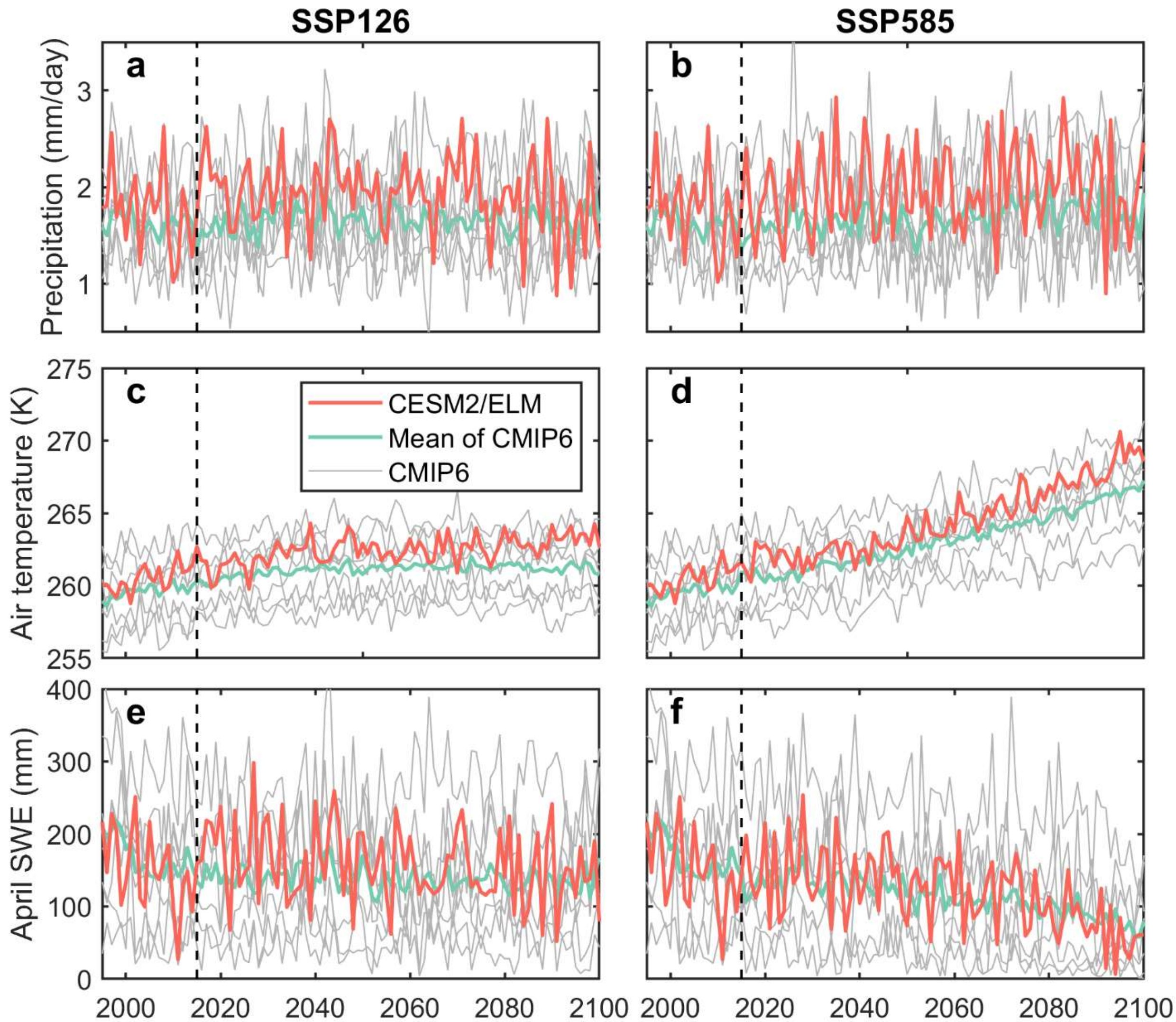

Figure S7| Time Series of (a,b) winter precipitation, (c,d) winter air temperature, and (e,f) April SWE over snow-covered TP regions (where the average SWE exceeds 5 mm in the historical period of 1995-2014) under (a,c,e)SSP126 and (b,d,f) SSP585. For each panel, the legend 'CESM2/ELM' represents either CESM2 data (precipitation or air temperature) or ELM simulated SWE; 'Mean of CMIP6' represents the ensemble mean of the seven CMIP6 models (Table S1) used in the study; 'CMIP6' represents each CMIP6 model used in the study; and the vertical dashed line indicates the year 2015 when the SSP scenarios start.

Table S1| Historical and future surface radiative forcings (RFs) from December to May induced by BC, dust, and BC+dust (i.e., the sum of BC and dust) over the snow-covered regions (where the average SWE exceeds 5 mm in the historical period of 1995-2014) in the NH and TP in ELM control simulations.

LAP	NH			TP		
	Historical	SSP126	SSP585	Historical	SSP126	SSP585
BC	0.79	0.13	0.17	3.16	0.57	0.61
Dust	0.37	0.49	0.28	1.24	1.58	0.69
BC+dust	1.3	0.65	0.49	5.13	2.39	1.47

Table S2| Details of seven Earth system models in the CMIP6 experiments used in the study.

Model Name	Institute/Center	Original spatial resolution (longitude × latitude)	Reference
CanESM5	Canadian Centre for Climate Modelling and Analysis, Canada	2.8° × 2.8°	Swart et al.[1]
CESM2	National Center for Atmospheric Research, USA	1.25° × 0.94°	Danabasoglu et al.[2]
GFDL-ESM4	Geophysical Fluid Dynamics Laboratory, USA	1.25° × 1.0°	Held et al.[3]
INM-CM5-0	Institute of Numerical Mathematics of the Russian Academy of Sciences, Russia	2.0° × 1.5°	Volodin et al.[4]
MIROC6	Japanese modeling community, Japan	1.4° × 1.4°	Tatebe et al.[5]
MRI-ESM2-0	Meteorological Research Institute, Japan	1.9° × 1.9°	Yukimoto et al.[6]
NorESM2-LM	Norwegian Climate Center, Norway	2.5° × 1.9°	Seland et al.[7]

Table S3| ELM-based experiments with different model configurations. TOP and PP represent the shortwave radiation parameterizations with and without considering the topographic effects on solar radiation. MSE represents the melt-water scavenging efficiency of hydrophilic BC.

Case ID	**Topographic effects on solar radiation**	**Snow grain shape**	**Mixing state of Hydrophilic-snow**	**Mixing state of dust-snow**	**Land use and land cover change**	**MSE**
Control	TOP	Spherical	Internal	External	Yes	0.2
PP	PP	Spherical	Internal	External	Yes	0.2
Koch	TOP	Koch Snowflake	Internal	External	Yes	0.2
extBC	TOP	Spherical	External	External	Yes	0.2
intDust	TOP	Spherical	External	Internal	Yes	0.2
noLULCC	TOP	Spherical	Internal	External	No	0.2
MSE_high	TOP	Spherical	Internal	External	Yes	2
MSE_low	TOP	Spherical	Internal	External	Yes	0.02

References

1. Swart NC, Cole JNS, Kharin VV, Lazare M, Scinocca JF, Gillett NP*, et al.* The Canadian Earth System Model version 5 (CanESM5.0.3). *Geosci Model Dev* 2019, **12**(11)**:** 4823-4873.

2. Danabasoglu G, Lamarque J-F, Bacmeister J, Bailey DA, DuVivier AK, Edwards J*, et al.* The Community Earth System Model Version 2 (CESM2). *Journal of Advances in Modeling Earth Systems* 2020, **12**(2)**:** e2019MS001916.

3. Held IM, Guo H, Adcroft A, Dunne JP, Horowitz LW, Krasting J*, et al.* Structure and Performance of GFDL's CM4.0 Climate Model. *Journal of Advances in Modeling Earth Systems* 2019, **11**(11)**:** 3691-3727.

4. Volodin E, Gritsun A. Simulation of observed climate changes in 1850–2014 with climate model INM-CM5. *Earth Syst Dynam* 2018, **9**(4)**:** 1235-1242.

5. Tatebe H, Ogura T, Nitta T, Komuro Y, Ogochi K, Takemura T*, et al.* Description and basic evaluation of simulated mean state, internal variability, and climate sensitivity in MIROC6. *Geosci Model Dev* 2019, **12**(7)**:** 2727-2765.

6. Yukimoto S, Kawai H, Koshiro T, Oshima N, Yoshida K, Urakawa S*, et al.* The Meteorological Research Institute Earth System Model Version 2.0, MRI-ESM2.0: Description and Basic Evaluation of the Physical Component. *Journal of the Meteorological Society of Japan Ser II* 2019, **97**(5)**:** 931-965.

7. Seland Ø, Bentsen M, Olivié D, Toniazzo T, Gjermundsen A, Graff LS*, et al.* Overview of the Norwegian Earth System Model (NorESM2) and key climate response of CMIP6 DECK, historical, and scenario simulations. *Geosci Model Dev* 2020, **13**(12)**:** 6165-6200.